Kinetics of the reaction between the antioxidant Trolox® and the free radical DPPH• in semi-aqueous solution†

Ouided Friaa and Daniel Brault*

Received 13th February 2006, Accepted 25th April 2006
First published as an Advance Article on the web 12th May 2006
DOI: 10.1039/b602147f

Reaction of the free-radical diphenylpicrylhydrazyl (DPPH•) with Trolox® (TrOH) was investigated in buffered hydroalcoholic media by using a stopped-flow system. DPPH• was reduced to the hydrazine analogue DPPH-H with a measured stoichiometry of about 2. DPPH-H was characterized by an acid–base equilibrium ($pK_a = 8.6$). Time-resolved absorption spectra recorded with an excess of either TrOH or DPPH• indicated that no significant amount of the TrO• radical was accumulated. The TrO• radical formed in a first step further reacted quickly with DPPH•. For 1 : 1 ethanol–buffer mixtures at pH 7.4, the bimolecular rate constants of the first and second steps were 1.1×10^4 M^{-1} s^{-1} and 2×10^6 M^{-1} s^{-1}, respectively. A significant increase of the measured rate constant was observed for ethanol–buffer solutions as compared to ethanol. The rate was also increased at higher pH. A deuterium isotopic effect of 2.9 was measured. These data are discussed with regards to mechanisms involving either electron or proton exchange as rate determining steps in the reaction of DPPH• with Trolox®. The importance of solvent acidity control in investigation of antioxidant properties is outlined.

Introduction

Scavenging deleterious radical species and redox status regulation are essential processes in normal cellular life.[1,2] Pathological states, and to some extent ageing, appear to be related to a deficiency in regulation leading to oxidative damage, a phenomenon known as oxidative stress.[3] Cells have set up various lines of defense, in particular to protect their membranes. Vitamin E inhibits chain peroxidation of polyunsaturated lipids by scavenging free-radicals.[4] It is present as α-tocopherol (α-TOH) in cell membranes where it is anchored by a lipophilic chain. This antioxidant, belonging to the hydroxychroman class, finds its efficacy in the reactivity of its phenolic group according to the overall reaction,

$$\alpha\text{-TOH} + \text{LOO}^{\bullet}\ (\text{or L}^{\bullet}) \rightarrow \alpha\text{-TO}^{\bullet} + \text{LOOH (or LH)} \qquad (1)$$

and to the relative stability of the α-tocopherol radical formed.[5] Indeed, α-TO• may recombine or disproportionate through reaction with another α-TO• radical, or may react with another LOO• radical. Thus, radical-chain peroxidation is stopped through the formation of non-radical products. Alternatively, α-TOH may be regenerated by reaction with another antioxidant, such as ascorbic acid.[6] Deleterious prooxidant conditions may develop when the α-tocopherol radical is not inactivated.[7] The importance of these reactions has prompted numerous studies to understand the reaction mechanism of hydroxychromans and other antioxidants belonging to the phenol and flavonoid classes. Antioxidants may react by a direct hydrogen atom transfer involving the labile hydrogen of phenol-like groups. This mechanism has gained support from the deuterium kinetic isotope effect[8,9] and the retardation of the reaction in solvents establishing a hydrogen bond with the H-atom of the phenol group.[10] This mechanism, referred to as HAT in recent literature,[11,12] is likely to be favored in apolar media such as the lipidic core of membranes, which can be mimicked by alkanes.[10] Alternatively, antioxidants may react through electron transfer concerted with, or followed by, proton transfer.[13,14] Besides, owing to its lower redox potential, the deprotonated phenol form is much more reactive towards various oxidants.[15,16] Then, an alternative mechanism assumes that ionization of the phenol group precedes electron exchange[12,17,18] and was named[11,19] sequential proton loss electron transfer (SPLET). This mechanism, favored in ionizing solvents, was established by the addition of acid to the reaction medium in order to suppress phenol ionization and by kinetic analysis.[12,19] It was also pointed out that adventitious acids or bases present in the solvent, or acidification by the antioxidant itself when it bears carboxylic chains, have important effects on the antioxidant reaction rate.[12,17] Theoretical calculations of bond dissociation enthalpy and ionization potentials as a measure of hydrogen *versus* electron transfer capability of various antioxidants place α-tocopherol not only as the best hydrogen donor, but also in a good position as an electron donor.[20] In the case of Trolox®, the ionization of the carboxylic group in a water medium might favor electron transfer. Clearly, the study of such reactions requires proton activity control.

Various methods have been designed to measure antioxidant power.[21] Some involve production of transient radical species under steady state[22] or pulse conditions.[13,23] Besides, stable organic radicals leading to color changes upon reaction with antioxidants have received much attention.[24–26] The commercially available 2,2-diphenyl-1-picrylhydrazyl radical (DPPH•) is becoming widely used.[12,17,27] It is reduced by antioxidants to the hydrazine form (DPPH-H). The colorimetric DPPH• method is particularly useful

Laboratoire de Biophysique Moléculaire Cellulaire et Tissulaire (BIOMOCETI) CNRS UMR 7033, Université Pierre et Marie Curie, Genopole Campus 1, 5 rue Henri Desbruères, 91030, Evry cedex, Paris, France. E-mail: dbrault@ccr.jussieu.fr; Fax: +33 1 69 87 43 60

† Electronic supplementary information (ESI) available: Absorption spectra taken in pH 6.4 and 8.4 buffers and in pure ethanol. See DOI: 10.1039/b602147f

to determine stoichiometric data, *i.e.* the number of radicals inactivated by one molecule of antioxidant. However, as protection against oxidative stress relies on a dynamic competition between the scavenging of radicals and their harmful reactions, kinetic data are most precious.[28]

Trolox®, a water-soluble α-tocopherol analogue with a carboxylic group replacing the lipophilic tail[23] is frequently used as an antioxidant standard. Obviously, sound knowledge of its reaction mechanism is required in order to use it as a reference.

In a continuation of the above-mentioned studies aimed to clarify the reaction mechanism of phenol-type antioxidants, we report on a UV-visible study of the reaction of Trolox® with DPPH• in ethanol–buffer mixtures allowing pH control. Focus is given on kinetic aspects. The influence of water content and deuterium isotopic effects are examined.

Results

Solution properties of compounds under study

Absorption spectra of TrOH, DPPH• and DPPH-H in 1 : 1 mixtures of ethanol with water buffered at pH 7.4 are reported in Fig. 1. Similar spectra were recorded for 1 : 1 mixtures buffered with water at pH 6.4 and 8.4 except for DPPH-H, which displays a pH dependent spectrum as reported below. The spectrum of DPPH-H at pH 8.4 is also depicted in Fig. 1.

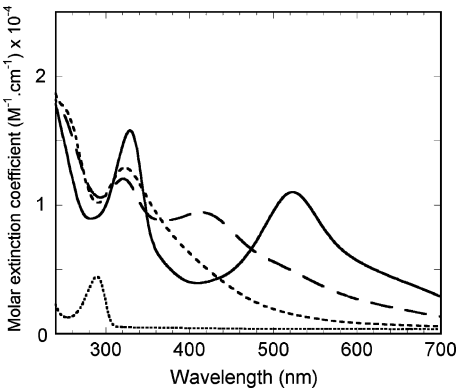

Fig. 1 Absorption spectra of Trolox® (···), DPPH• (—), DPPH-H (---) in 1 : 1 ethanol–pH 7.4 buffer mixture and DPPH-H (— —) in the same solution, except that the buffer was adjusted to 8.4.

Solutions of TrOH, DPPH• and DPPH-H were found to obey Beer's law at least up to 2×10^{-3}, 1.4×10^{-4} and 1.1×10^{-4} M, respectively. Beer's law was also obeyed in all the other ethanol–water mixtures. The absorption maximum of DPPH• was found at 524 nm with a molar extinction coefficient, ε, of 10700 ± 500 M^{-1} cm^{-1} in 1 : 1 ethanol–buffer mixtures at all pH values. In pure ethanol the maximum was at 515 nm (ε = 10600 ± 200 M^{-1} cm^{-1}). Trolox® presents a band at 290 nm (ε = 3000 ± 100 M^{-1} cm^{-1}) in all the 1 : 1 ethanol–buffer mixtures.

The spectral dependence of DPPH-H solutions in 1 : 1 ethanol–water mixtures between pH 6.1 and 9.6 is illustrated in Fig. 2a. At the lowest pH, DPPH-H presents a band at 323 nm. When the pH is increased, a slight decrease and blue shift of this band is observed and, more prominently, an intense band at 426 nm

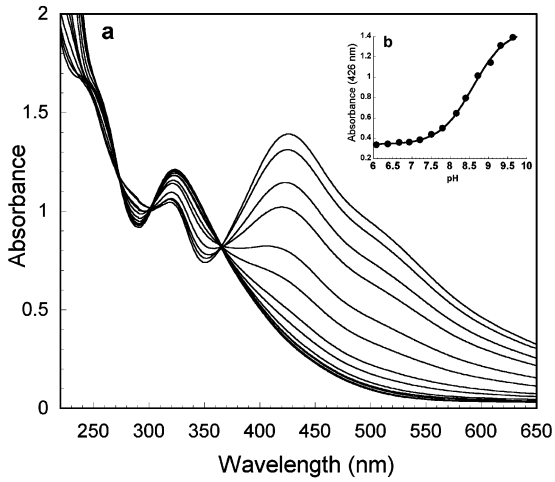

Fig. 2 (a) Absorption spectra of DPPH-H (8.3×10^{-5} M, 1 : 1 ethanol–buffer solutions) at various pH: 6.1 (bottom), 6.4, 6.7, 6.9, 7.2, 7.5, 7.8, 8.2, 8.4, 8.7, 9.0, 9.3, 9.6 (top). (b) Absorbance at 426 nm *versus* pH. The full line corresponds to the theoretical fit (see text) for a pK value of 8.59.

appears. Nice isosbestic points are observed at 365 and 302 nm. These changes suggest an acid–base equilibrium according to:

$$\text{DPPH-H} \rightleftarrows \text{DPPH}^- + \text{H}^+ \quad (2)$$

The absorbance at 426 nm (Abs) was fitted by using non-linear curve method according to the equation:

$$\text{Abs} = [\text{Abs}_{\text{AH}} + \text{Abs}_{\text{A}} \times 10^{(\text{pH}-\text{p}K)}]/(1 + 10^{(\text{pH}-\text{p}K)})$$

where Abs_{AH} and Abs_{A} are the absorbances of the pure acid (DPPH-H) and basic (DPPH^-) forms, respectively. The fit displayed in Fig. 2b allowed us to derive a pK of 8.59 ± 0.03, a value in good agreement with literature data.[29]

Reaction of DPPH• with TrOH

Either TrOH or DPPH• were used in excess in order to analyze kinetics under pseudo-first order conditions.[30]

TrOH in excess

A typical set of spectra recorded after mixing solutions of DPPH• (7.7×10^{-5} M after mixing) and TrOH (7.75×10^{-4} M after mixing) in 1 : 1 ethanol–buffer mixtures at pH 7.4 is displayed in Fig. 3a. The reaction was completed within 2.4 s. It was found to correspond to the consumption of all the DPPH• present to yield the DPPH-H form, as ascertained by comparison with spectra of the pure compounds.

Solutions made with buffers at pH 6.4 yielded about the same sets of spectra (see the ESI). The spectral changes recorded with buffer at pH 8.4 (see the ESI) show a larger absorbance increase of around 420 nm. This was due to the contribution of the deprotonated form of the hydrazine, DPPH^-, according to the above-mentioned acid–base equilibrium (eqn 2). This is believed to be established quickly, as is usual for proton exchange reactions.[31]

Difference spectra obtained by subtracting the first recorded spectrum from subsequent spectra are shown in Fig. 3b. They allow better inspection of isosbestic points that appear to be clearly

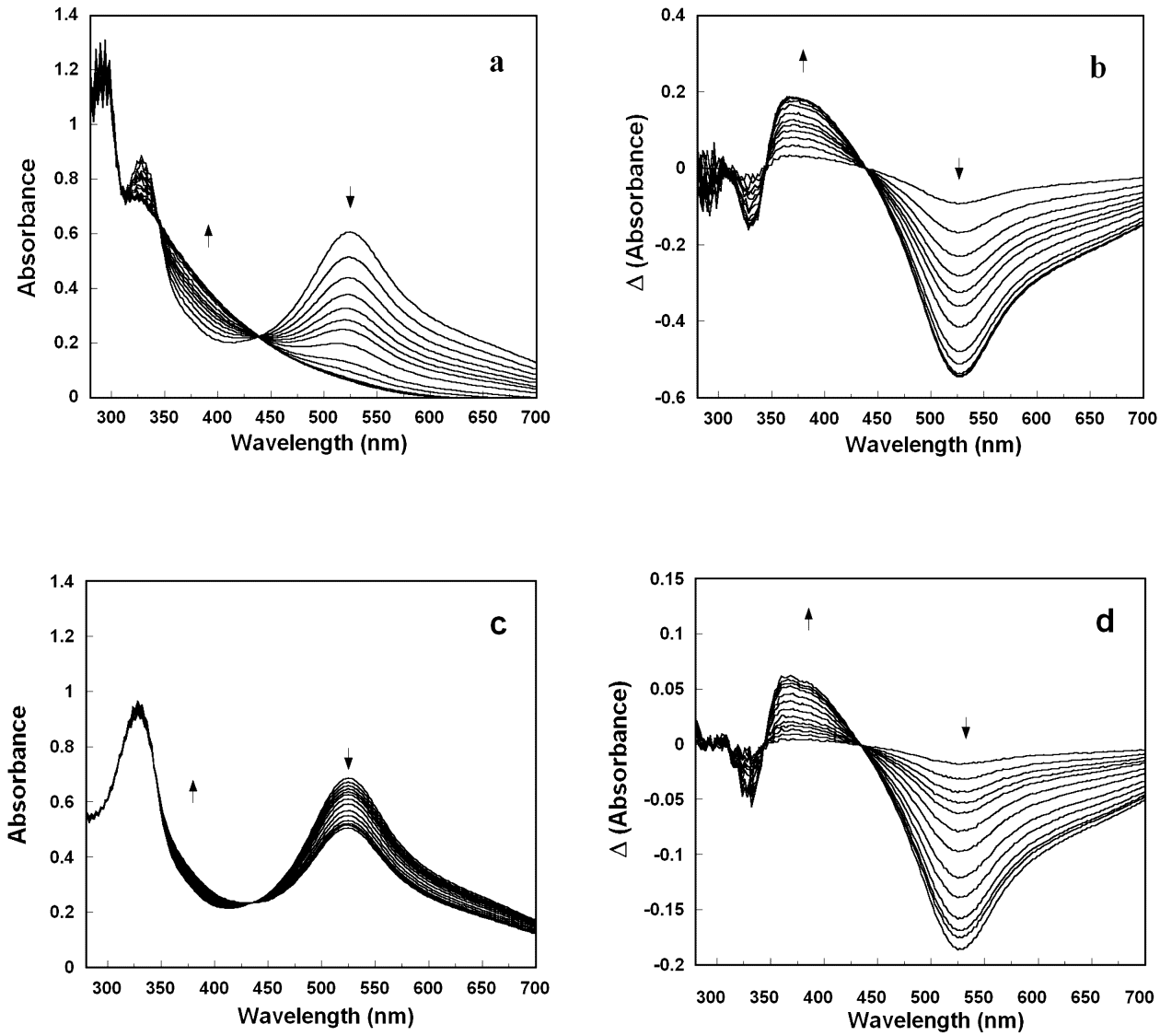

Fig. 3 Time dependence of DPPH$^{\bullet}$ absorption spectra upon reaction with TrOH in 1 : 1 ethanol–pH 7.4 buffer mixture. (a–b) DPPH$^{\bullet}$: 7×10^{-5} M, TrOH: 7.75×10^{-4} M (excess). Times after mixing: 0.006, 0.018, 0.030, 0.042, 0.055, 0.067, 0.079, 0.103, 0.152, 0.201, 0.310, 0.407, 0.492, 0.809, 1.00, 1.50, 2.43 s. (c–d) DPPH$^{\bullet}$: 7.5×10^{-5} M (excess), TrOH: 7.8×10^{-6} M. Times after mixing, 0.049, 0.146, 0.243, 0.340, 0.438, 0.535, 0.730, 1.02, 1.51, 2.09, 3.06, 4.04, 5.01, 10.07 s. Difference spectra in panels (b) and (d) are derived from absolute spectra by subtracting the initial spectrum to subsequent spectra. The arrows indicate direction of the absorption changes.

conserved. For 1 : 1 mixtures buffered at pH 7.4 these points are observed at 345 and 439 nm. Similar findings were obtained for 1 : 1 mixtures buffered at pH 6.4 and 8.4 as well as for pure ethanol (see the ESI).

The kinetics of the reaction were analyzed in more detail at specific wavelengths. The decrease of DPPH$^{\bullet}$ absorption at 524 nm in a 1 : 1 mixture of ethanol and buffer (pH 7.4) is shown in Fig. 4.

In this experiment, TrOH (9.06×10^{-4} M) was in large excess as compared to DPPH$^{\bullet}$ (5.33×10^{-5} M). The process appears to be mainly monophasic and was tentatively fitted by an exponential. The fit and residuals (curve fit minus experimental data) are displayed in Fig. 4. Agreement was found to be fairly good, although not perfect as shown by some fluttering observed on the residuals. The fluttering was somewhat increased for lower TrOH : DPPH$^{\bullet}$ ratios. The observed rate constant derived from monoexponential fit was found to linearly depend on the TrOH concentration as shown in Fig. 5a. As depicted in Fig. 5b, these slopes increase with pH. For instance, they were found to be 17200 ± 700, 18200 ± 800 and 31200 ± 3400 M^{-1} s^{-1} at pH 6.4, 7.4 and 8.4, respectively.

Similar kinetic traces were obtained in mixtures made with lower water content. The slopes of the linear fit were significantly lower, however. For 2 : 1 and 3 : 1 ethanol–water mixtures, slopes were found to be 5700 ± 100 and 4200 ± 100 M^{-1} s^{-1} at pH 6.7, 8600 ± 1300 and 7000 ± 700 M^{-1} s^{-1} at pH 7.4, 10200 ± 800 and 7600 ± 300 M^{-1} s^{-1} at pH 8.4, respectively. In pure ethanol (data not shown), the slope of the linear fit was much lower, 320 ± 5 M^{-1} s^{-1}.

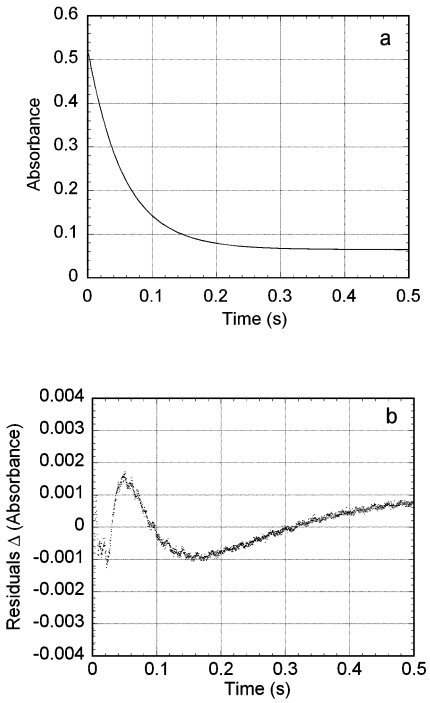

Fig. 4 (a) Absorbance decay ($\lambda = 524$ nm) following mixing of DPPH$^{\bullet}$ (5.33×10^{-5} M after mixing) and TrOH (9.06×10^{-4} M) in 1 : 1 ethanol–buffer solutions (pH 7.4). (b) Residuals (curve fit minus experimental data) from monoexponential fit.

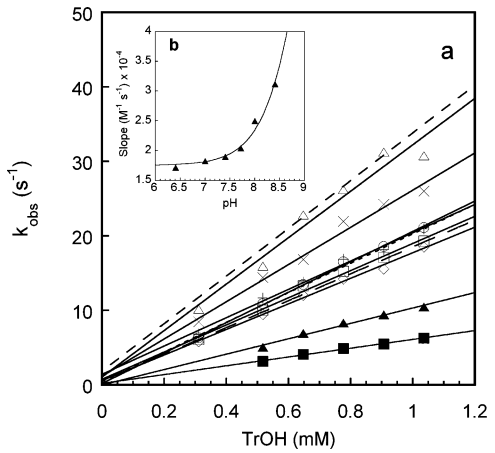

Fig. 5 (a) Linear dependence (solid lines) of the observed rate constants on Trolox® concentration at pH (◆) 6.4, (□) 7.0, (+) 7.4, (○) 7.7, (×) 8.0, (△) 8.4 and pD (■) 7.4, (▲) 8.8. Dependence of simulated rate constants (see text) on Trolox® concentration at pH 6.4 (— —), 7.4 (- - -) and 8.4 (– – –). (b) Slopes of the linear plots shown in panel (a) *versus* pH.

Deuterium isotopic effect

Deuterated hydroalcoholic solutions were prepared by mixing deuterated ethanol with an equal volume of deuterium oxide buffered to pD 7.4 or 8.8. Fairly good fits to the monoexponentials were obtained in both cases and the observed rate constants thus derived were found to linearly depend on Trolox® concentration, as shown in Fig. 5a. The bimolecular rate constants were significantly lower than those for non-deuterated medium.

DPPH$^{\bullet}$ in excess

Spectra were recorded after mixing solutions of DPPH$^{\bullet}$ (7.5×10^{-5} after mixing) and TrOH (7.8×10^{-6} M after mixing) in 1 : 1 ethanol–buffer mixtures at various pH. In this case, the TrOH concentration is the limiting factor and DPPH$^{\bullet}$ is only partly consumed. Spectral changes obtained with solutions made with pH 7.4 buffer are displayed in Fig. 3c along with difference spectra calculated as above (Fig. 3d). Quite well-defined isosbestic points were observed at 346 and 453 nm. These difference spectra are similar to those recorded with excess TrOH, except that the isosbestic points were somewhat shifted. Solutions made with buffers at pH 6.4 and 8.4 yielded about the same sets of spectra (see the ESI).

The stoichiometry of the reaction, n, was calculated by using the relation $n = \Delta(\text{Abs})/(\Delta\varepsilon \times l \times [\text{TrOH}])$ where Δ(Abs) is the absorbance change recorded at the end of the reaction for a given wavelength, $\Delta\varepsilon$ is the difference between the molar extinction coefficients of DPPH$^{\bullet}$ and DPPH-H, l is the optical length of the optical cell and [TrOH] the Trolox® concentration. Changes in the DPPH-H spectrum with pH were taken into account in the calculation. The stoichiometry was found to be 2.50 ± 0.05, 2.10 ± 0.05 and 1.8 ± 0.07 at pH 6.4, 7.4 and 8.4, respectively. These values correspond to the mean of four measurements on solution containing DPPH$^{\bullet}$ and TrOH in ratios between 10 and 20.

Discussion

The reaction of the colored DPPH$^{\bullet}$ radical is a popular method to evaluate the strength of antioxidants. We have investigated kinetic aspects of this reaction with a water-soluble analogue of vitamin E, Trolox®, commonly used as a standard. In keeping with current knowledge from the literature, the reaction is described by the scheme shown in Fig. 6.

DPPH$^{\bullet}$ being a free radical, the initial step of the reaction with Trolox® leads to the formation of the one-electron oxidized form of the antioxidant, the phenoxyl-type radical TrO$^{\bullet}$. This first step could be reversible, as suggested for phenols.[32] The TrO$^{\bullet}$ radical can react with remaining DPPH$^{\bullet}$ (line (b) of the scheme in Fig. 6) or disappears through dimerization or disproportionation reactions involving resonant forms[33] [line (c)].

The TrO$^{\bullet}$ radical possesses an absorption band around 435 nm in water[23] very close to the isosbestic points observed in Fig. 3 (see also the ESI for the other pH values). We can estimate that a variation of 10% of the absorbance at these specific wavelengths should be visible on the difference spectra. We will take the spectra shown in Fig. 3a–b as an example. In this experiment, the maximum concentration of TrO$^{\bullet}$ that could be formed is equal to the DPPH$^{\bullet}$ concentration (the limiting reagent), *i.e.* 7.7×10^{-5} M. An isosbestic point is observed at 439 nm with an absorbance of 0.22. At this wavelength, the molar extinction coefficient of the Trolox® radical is 7000 M^{-1} cm^{-1} according to published data.[23] Thus, it can be estimated that change in the concentration of the TrO$^{\bullet}$ radical in the course of the reaction does not exceed about 3×10^{-6} M, *i.e.* 5% of the maximum value.

The system can be described by the following set of differential equations:

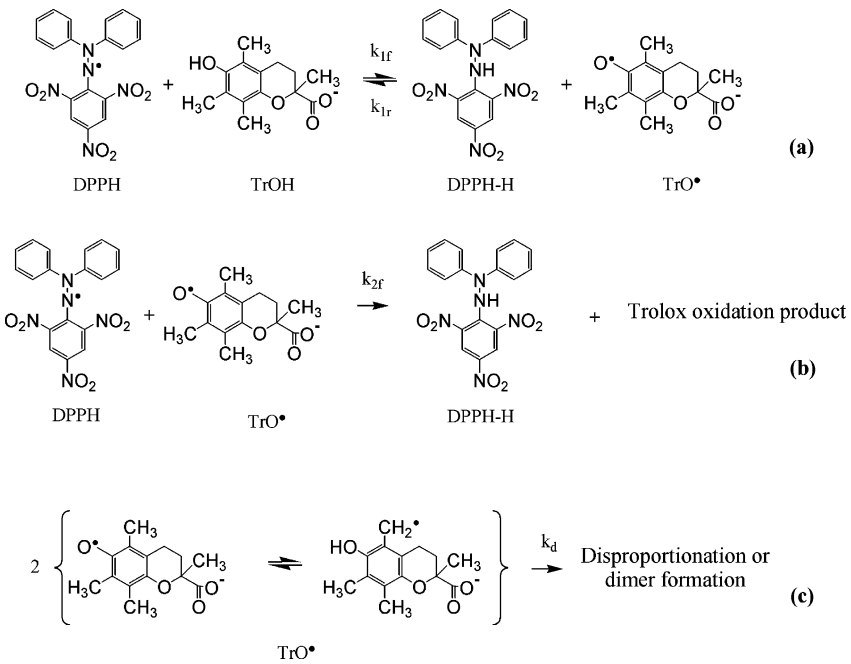

Fig. 6 Postulated reaction scheme of the reaction between DPPH• and Trolox®. In the pH range investigated, Trolox® is present as its carboxylate form as shown in the scheme.

$$d[DPPH^{\bullet}]/dt = -k_{1f} \times [DPPH^{\bullet}] \times [TrOH] + k_{1r} \times [DPPH\text{-}H] \times [TrO^{\bullet}] - k_{2f} \times [DPPH^{\bullet}] \times [TrO^{\bullet}]$$

$$d[TrOH]/dt = -k_{1f} \times [DPPH^{\bullet}] \times [TrOH] + k_{1r} \times [DPPH\text{-}H] \times [TrO^{\bullet}]$$

$$d[DPPH\text{-}H]/dt = k_{1f} \times [DPPH^{\bullet}] \times [TrOH] - k_{1r} \times [DPPH\text{-}H] \times [TrO^{\bullet}] + k_{2f} \times [DPPH^{\bullet}] \times [TrO^{\bullet}]$$

$$d[TrO^{\bullet}]/dt = k_{1f} \times [DPPH^{\bullet}] \times [TrOH] - k_{1r} \times [DPPH\text{-}H] \times [TrO^{\bullet}] - k_{2f} \times [DPPH^{\bullet}] \times [TrO^{\bullet}] - 2 \times k_{d} \times [TrO^{\bullet}]^2$$

It was not possible to obtain an analytical mathematical solution for this system. A short program based on these differential equations and on rate constant estimates was thus written for the Mathcad software. For each initial Trolox® and DPPH• concentrations, the program yielded the TrO• and DPPH• concentrations as a function of time for various sets of estimates for the $2 \times k_d$, k_{1f} and k_{2f} rate constants. The bimolecular rate constant, $2 \times k_d$, has been estimated to be 4×10^5 M^{-1} s^{-1} in pH 7.4 buffer.[34] This value was introduced as a constant in the program. The above-mentioned limit for the change in the TrO• concentration was used as a constraint to select valid rate constant sets. The curves simulating the DPPH• concentration were fitted to monoexponentials. The exponential factor obtained from the simulation was compared to the experimental rate constant and the set of k_{1f} and k_{2f} constants adjusted in order to obtain the best agreement over the whole range of the Trolox® concentration. Fluttering of the residuals similar to those depicted in experimental curves (see Fig. 4b) was accepted. The reversibility of the reaction was also checked. In fact, reversibility requires the introduction of a k_{1r} constant with a high enough value. However, this led to decay curves significantly departing from the exponential, suggesting that the back reaction is unimportant in our experimental conditions. Therefore, this constant was kept low enough and had no effect on the simulation. The result of such simulation is illustrated in Fig. 5a for pH 7.4 solutions. A good agreement was found between simulated and experimental data by using $k_{1f} = 1.1 \times 10^4$ M^{-1} s^{-1} and $k_{2f} = 2 \times 10^6$ M^{-1} s^{-1}. The value of the dimerization constant, $2 \times k_d = 4 \times 10^5$ M^{-1} s^{-1}, was also found to be a reasonable estimate. Similar agreement was found at pH 6.4 and 8.4 with the values $k_{1f} = 1.0 \times 10^4$ M^{-1} s^{-1}, $k_{2f} = 2 \times 10^6$ M^{-1} s^{-1} and $k_{1f} = 1.9 \times 10^4$ M^{-1} s^{-1}, $k_{2f} = 2 \times 10^6$ M^{-1} s^{-1}, respectively. It can be noted that the rate constant k_{2f} is quite large. The stoichiometry of the reaction measured with DPPH• in excess was found to be close to the value of 2 in agreement with the sequence of reactions described in line (a) and (b) of the scheme in Fig. 6.

As depicted in Fig. 5b, the observed rate constant for the reaction of DPPH• with excess Trolox® increases with pH. The Trolox® carboxylic chain with a pK of 3.6 in water[35] is not likely to be directly involved. In fact, in all cases, Trolox® is expected to be present as its carboxylate form as depicted in Fig. 6. It could be hypothesized that a form of the Trolox® radical protonated on the phenol ($TrOH^{\bullet+}$) is first produced through reaction with DPPH•. The overall reaction would be accelerated upon deprotonation of this form. The pK_a for the $TrOH^{\bullet+}/TrO^{\bullet}$ couple has been estimated[36] to be 2.3. This value appears too low as compared to the pH range investigated to sustain this hypothesis, that was also rejected by Litwinienko.[37] Alternatively, this effect may arise from deprotonation of the phenol group, the pK of which has been estimated[15,23] to range between 11.9 and 11.7. As shown by pulse radiolysis studies, phenolate ions react with various oxidizing radicals much more quickly than phenols.[15] The same effect was found when singlet oxygen was used as an oxidizing agent.[16] Based on the higher reactivity of the phenolate form, a sequential proton loss electron transfer (SPLET) mechanism was recently proposed by Litwinienko[11,19,37] and Foti.[12] Unfortunately, the poor stability

of DPPH$^{\bullet}$ above pH 9.0 did not allowed us to investigate the pH effect over a large range.

Our value for the rate constant of the reaction between DPPH$^{\bullet}$ and Trolox® in pure ethanol (320 M^{-1} s^{-1}) is fairly similar to that reported for methanol solutions[38] (360 M^{-1} s^{-1}). For comparison, another tocopherol analog, pentamethylhydroxychroman, yielded similar values in ethanol (410 M^{-1} s^{-1})[37] and values ranging between 350 M^{-1} s^{-1} and 1070 M^{-1} s^{-1} in methanol.[14,37] An important acceleration of the reaction is observed when ethanol–water mixtures are used instead of pure ethanol, in favor of an electron transfer process. Deuterium isotopic effect has been investigated to shed some light on the mechanism. In fact, deuterium substitution may have several consequences. First, in a pure hydrogen abstraction process involving a linear transition state, it is expected that the rate would be decreased by a factor equal to the relative vibrational energy of the O–H and O–D bonds, *i.e.* 9.8. This value was approached for the reaction of DPPH$^{\bullet}$ with phenols in pure benzene.[39] In aqueous solutions, the ionization of the phenol group must be taken into account as outlined above. The acidity of the phenol group is likely to be reduced in D_2O. Typically, weak acids are weaker in D_2O than in H_2O by about 0.4–0.5 pK units.[40,41] In our experiments, the buffers were adjusted to pD values of 7.4 and 8.8. Thus, the ionization states of the phenol group, and eventually of reaction intermediates, would be similar to those in non-deuterated mixtures at pH 7.0 and 8.4. The slopes of the curves reported in Fig. 5a were compared accordingly. An isotopic effect of 2.9 ± 0.3 was measured for the two pH/pD values. Even if lower than that reported for a pure organic solvent,[39] this isotopic effect is significant. The reason of this effect cannot be found in a difference of the initial ionization state of Trolox®, as outlined above. It can be hypothesized that the rate of deprotonation of the phenol group could be a limiting factor. This interpretation is in line with the SPLET mechanism. Alternatively, a former study on the reaction of radicals with organic reductants by Neta[13] suggested that electron and proton transfer involving the solvent could be concerted in the transition state. A kinetic isotopic effect of about 2 was found in this study.[13] A mechanism involving concerted proton transfer to the incipient DPPH anion in the transition state is possible and would be consistent with the measured isotopic effect.

Noticeably, the increase of the slope in Fig. 5 is about twofold for one pH unit change, whereas a tenfold increase would be expected for a process entirely controlled by phenol group deprotonation. At the lowest pH, the slope tends to a constant value of 1.75×10^4 M^{-1} s^{-1}. It could be assumed that the SPLET mechanism[11,12,17,19,37] would be favored in the highest pH range while proton-transfer-mediated electron transfer[13] would dominate at the lowest pH.

In conclusion, our results, taken together with literature data,[12,17] highlight the importance of the control of solvent acidity. Obviously, this is better achieved by using mixtures of an aqueous buffer with a miscible organic solvent. These systems would allow studies of a large panel of antioxidants with various water solubility properties and should help the characterization of natural and synthetic antioxidants.[42,43] Furthermore, they may provide a better insight into the complex mechanism of antioxidant reactions. Also, kinetics should be considered in order to understand how antioxidants could inhibit the development of the radical reaction responsible for oxidative stress. The present study is likely to help in the development of research on other antioxidants in these directions.

Materials and methods

Materials

The stable free-radical 2,2-diphenyl-1-picrylhydrazyl (DPPH$^{\bullet}$), 95% pure and 6-hydroxy-2,5,7,8-tetramethylchroman-2-carboxylic acid (Trolox®, TrOH), 97% pure were purchased from Sigma-Aldrich (Saint-Quentin Fallavier, France) and 1,1-diphenyl-2-picrylhydrazine, (DPPH-H), 98% pure from Fluka Chemika (Buchs, Switzerland). Stock solutions of these compounds were made in analytical grade ethanol from Merck (VWR, Fontenay-sous-Bois, France) and stored at 4 °C for a maximum of 2 d in the dark. DPPH$^{\bullet}$ and DPPH-H dissolve slowly in ethanol. Ethanol-d (99.5% deuteration) was purchased from Sigma-Aldrich and deuterium oxide (99.9% D) from Eurisotop (Saclay, France). Ultra-pure water was furnished by a Direct-Q3 apparatus from Millipore (Molsheim, France).

Hydroalcoholic mixtures were prepared by adding ethanol to the desired amount (*v*/*v*) of water that was previously buffered at the desired pH. Tris(hydroxymethyl)aminomethane (TRIS) or bis(2-hydroxyethyl)iminotris(hydroxymethyl)methane (BIS-TRIS) at a concentration of 10 mM in the aqueous component were used in the pH range 7.4–9.6 and 6.1–7.2, respectively. TRIS and BIS-TRIS were purchased from Merck and Sigma-Aldrich, respectively. For deuterium isotopic experiments, the heavy water component was buffered by using 10 mM of TRIS or BIS-TRIS for "pH" 8.4 and 7.0, respectively. These "pH" values correspond to the reading of the glass electrode standardized in the usual way. The pD values were calculated according to Salomaa by adding 0.4 units to these "pH" values.[40] In all cases, solutions were normally equilibrated with air.

Instruments

The pH of the aqueous solutions was measured with a Radiometer PHM240 apparatus (Radiometer Analytical, Villeurbanne, France) equipped with a glass electrode and calibrated with standards from Radiometer. UV-visible absorption spectra were recorded with a UVIKON 923 spectrophotometer (Bio-Tek, Kontron Instrument, Milano, Italy). An Applied Photophysics (Leatherhead, UK) stopped-flow apparatus (model SX 18MV) equipped with a 150 W xenon arc lamp was used for kinetic measurements and to record time-resolved spectra. The mixing time was 1.2 ms. Equal volumes of DPPH$^{\bullet}$ and Trolox® solutions, made with the same ethanol–water proportion, were mixed. Absorption changes at a single wavelength were recorded by using a conventional photomultiplier over total times ranging from 2.4 to 40 s. Typically, kinetic traces were composed of 2000 points and at least 4 signals were averaged. Time-resolved absorption spectra were collected in the range 200–740 nm by using a photodiode array with a resolution of 2.17 nm. At the maximum scan speed (2.56 ms between spectra) the first spectrum can be recorded 3.76 ms after the start of mixing. The slits were reduced to 0.8 mm in order to avoid DPPH$^{\bullet}$ photobleaching. Experiments were carried out at 20 °C.

Data were fitted either by using the software furnished by Applied Photophysics or Kaleidagraph from Synergy Software (Reading, PA, USA). The Levenberg–Marquard algorithm was used for non-linear curve fitting. The Mathcad software (Mathsoft, Inc., Cambridge, MA) was used for numerical simulations.

Acknowledgements

This work was supported by the charity associations "Fondation Marcel Bleustein-Blanchet pour la Vocation" and "Association pour la Recherche contre le Cancer" (ARC) through PhD grants to O.F. The stopped-flow apparatus was acquired thanks to subsidy from ARC (grant # 7209).

References

1 H. Sies, *Eur. J. Biochem.*, 1993, **215**, 213–219.
2 T. Finkel, *Curr. Opin. Cell Biol.*, 2003, **15**, 247–254.
3 B. Halliwell and J. M. C. Gutteridge, *Free radicals in biology and medicine*, 3rd edn, Oxford University Press, Oxford, 1999.
4 G. W. Burton and K. U. Ingold, *Acc. Chem. Res.*, 1986, **19**, 194–201.
5 G. W. Burton, T. Doba, E. Gabe, L. Hughes, F. L. Lee, L. Prasad and K. U. Ingold, *J. Am. Chem. Soc.*, 1985, **107**, 7053–7065.
6 J. E. Packer, T. F. Slater and R. L. Willson, *Nature*, 1979, **278**, 737–738.
7 V. W. Bowry and R. Stocker, *J. Am. Chem. Soc.*, 1993, **115**, 6029–6044.
8 P. B. Ayscough and K. E. Russell, *Can. J. Chem.*, 1965, **43**, 3039–3044.
9 G. W. Burton and K. U. Ingold, *J. Am. Chem. Soc.*, 1981, **103**, 6472–6477.
10 L. Valgimigli, J. T. Banks, K. U. Ingold and J. Lusztyk, *J. Am. Chem. Soc.*, 1995, **117**, 9966–9971.
11 G. Litwinienko and K. U. Ingold, *J. Org. Chem.*, 2004, **69**, 5888–5896.
12 M. C. Foti, C. Daquino and C. Geraci, *J. Org. Chem.*, 2004, **69**, 2309–2314.
13 P. Neta, R. E. Huie, P. Maruthamuthu and S. Steenken, *J. Phys. Chem.*, 1989, **93**, 7654–7659.
14 I. Nakanishi, T. Kawashima, K. Ohkubo, H. Kanazawa, K. Inami, M. Mochizuki, K. Fukuhara, H. Okuda, T. Ozawa, S. Itoh, S. Fukuzumi and N. Ikota, *Org. Biomol. Chem.*, 2005, **3**, 626–629.
15 S. Steenken and P. Neta, *J. Phys. Chem.*, 1982, **86**, 3661–3667.
16 R. Scurlock, M. Rougee and R. V. Bensasson, *Free Radical Res. Commun.*, 1990, **8**, 251–258.
17 G. Litwinienko and K. U. Ingold, *J. Org. Chem.*, 2003, **68**, 3433–3438.
18 I. Nakanishi, K. Miyazaki, T. Shimada, Y. Iizuka, K. Inami, M. Mochizuki, S. Urano, H. Okuda, T. Ozawa, S. Fukuzumi, N. Ikota and K. Fukuhara, *Org. Biomol. Chem.*, 2003, **1**, 4085–4088.
19 G. Litwinienko and K. U. Ingold, *J. Org. Chem.*, 2005, **70**, 8982–8990.
20 M. Leopoldini, T. Marino, N. Russo and T. M., *J. Phys. Chem. A*, 2004, **108**, 4916–4922.
21 K. Schlesier, M. Harwat, V. Bohm and R. Bitsch, *Free Radical Res.*, 2002, **36**, 177–187.
22 V. W. Bowry and K. U. Ingold, *J. Org. Chem.*, 1995, **60**, 5456–5467.
23 M. J. Davies, L. G. Forni and R. L. Willson, *Biochem. J.*, 1988, **255**, 513–522.
24 M. S. Blois, *Nature*, 1958, **181**, 1199–1200.
25 R. Re, N. Pellegrini, A. Proteggente, A. Pannala, M. Yang and C. Rice-Evans, *Free Radical Biol. Med.*, 1999, **26**, 1231–1237.
26 M. B. Arnao, *Trends Food Sci. Technol.*, 2000, **11**, 419–421.
27 W. Brand-Williams, M. E. Cuvelier and C. Berset, *Lebensm.-Wiss. Technol.*, 1995, **28**, 25–30.
28 P. Goupy, C. Dufour, M. Loonis and O. Dangles, *J. Agric. Food Chem.*, 2003, **51**, 615–622.
29 L. Constantin, P. Ionita and T. Constantinescu, *Rev. Roum. Chim.*, 1994, **39**, 1141–1150.
30 C. Capellos and B. H. J. Bielski, *Kinetic systems*, Wiley-Interscience, New York, 1972.
31 M. Eigen, W. Kruse, G. Maass and L. De Maeyer, in *Progress in reaction kinetics*, ed. G. Porter, Pergamon Press, Oxford, 1964, vol. 2, pp. 287–318.
32 J. S. Hogg, D. H. Lohmann and K. E. Russell, *Can. J. Chem.*, 1961, **39**, 1588–1594.
33 A. Kamal-Eldin and L. A. Appelqvist, *Lipids*, 1996, **31**, 671–701.
34 E. Nunez Delicado, A. Sanchez Ferrer and F. Garcia Carmona, *Biochim. Biophys. Acta*, 1997, **1335**, 127–134.
35 J. Malyszko and M. Mechanik, *Polish J. Chem.*, 2004, **78**, 1575–1582.
36 M. J. Thomas and B. H. J. Bielski, *J. Am. Chem. Soc.*, 1989, **111**, 3315–3319.
37 M. Musialik and G. Litwinienko, *Org. Lett.*, 2005, **7**, 4951–4954.
38 S. Santosh Kumar, K. I. Priyadarsini and K. B. Sainis, *Redox Rep.*, 2002, **7**, 35–40.
39 R. A. Bird, G. A. Harpell and K. E. Russell, *Can. J. Chem.*, 1962, **40**, 701–704.
40 P. Salomaa, L. L. Schaleger and F. A. Long, *J. Am. Chem. Soc.*, 1964, **86**, 1–7.
41 L. Melander and W. H. Saunders, *Reaction rates of isotopic molecules*, John Wiley & Sons, New York, 1980.
42 C. A. Rice-Evans, N. J. Miller and G. Paganga, *Free Radical Biol. Med.*, 1996, **20**, 933–956.
43 M. Roche, C. Dufour, N. Mora and O. Dangles, *Org. Biomol. Chem.*, 2005, **3**, 423–430.